Cadmium-transformed cells in the *in vitro* Cell Transformation Assay reveal different proliferative behaviours and activated pathways

Forcella M. [a#], Callegaro G. [b#], Melchioretto P.[b], Gribaldo L.[c], Frattini M.[d], Stefanini F.M.[e], Fusi P.[a*], Urani C.[b*]

[a] Department of Biotechnology and Biosciences, University of Milan Bicocca, Piazza della Scienza 3, 20126 Milan, Italy;
[b] Department of Earth and Environmental Sciences, University of Milan Bicocca, Piazza della Scienza 1, 20126 Milan, Italy;
[c] Institute for Health and Consumer Protection, DG JRC, European Commission, Via Enrico Fermi 2749, 21027 Ispra, Varese, Italy
[d] Istituto Cantonale di Patologia, Via in Selva 24, 6601 Locarno, Switzerland
[e] Department of Statistics, Computer Science, Applications, University of Florence, Viale Morgagni 59, 50100 Florence, Italy

[#] Matilde Forcella and Giulia Callegaro contributed equally to the work

Paola Fusi and Chiara Urani are co-last Authors

***Correspondence addresses:**

Paola Fusi
Department of Biotechnology and Biosciences
University of Milan Bicocca
Piazza della Scienza, 3
20126 Milan, Italy
Phone +39 0264483405
Fax +39 0264483565
e-mail: paola.fusi@unimib.it

Chiara Urani
Department of Earth and Environmental Sciences
University of Milan Bicocca
Piazza della Scienza, 1
20126 Milan, Italy
Phone +39 0264482923
Fax +39 0264482996
e-mail: chiara.urani@unimib.it

Abstract 200 words

The *in vitro* Cell Transformation Assay (CTA) is a powerful tool for mechanistic studies of carcinogenesis. The endpoint is the classification of transformed colonies (*foci*) by means of standard morphological features. To increase throughput and reliability of CTAs, one of the suggested follow-up activity is to exploit the comprehension of the mechanisms underlying cell transformation. To this end, we have performed CTAs testing $CdCl_2$, a widespread environmental contaminant classified as a human carcinogen with the underlying mechanisms of action not completely understood. We have isolated and re-seeded the cells at the end (6 weeks) of *in vitro* CTAs to further identify the biochemical pathways underlying the transformed phenotype of *foci*. Morphological evaluations and proliferative assays confirmed the loss of contact-inhibition and the higher proliferative rate of transformed clones. The biochemical analysis of EGFR pathway revealed that, despite the same initial carcinogenic stimulus (1μM $CdCl_2$ for 24 hours), transformed clones are characterized by the activation of two different molecular pathways: proliferation (Erk activation) or survival (Akt activation). Our preliminary results on molecular characterization of cell clones from different *foci* could be exploited for CTAs improvement, supporting the comprehension of the *in vivo* process and complementing the morphological evaluation of *foci*.

Keywords: cadmium; carcinogenesis; *in vitro* Cell Transformation Assay; epidermal growth factor receptor pathway.

1. INTRODUCTION

Cadmium (Cd) is a widespread environmental contaminat that has been shown to cause adverse health effects. The non-occupational exposure arises mainly from the diet, the ingestion of contaminated drinking-water, the inhalation of ambient air, and from contaminated soil or dust. Other possible sources of exposure are represented by phosphate-based fertilizers, and cosmetic products, in which Cd is used for its colour properties. In addition, in the general population, cigarettes represent a significant source due to a natural Cd accumulation by tobacco leaves. Once entered the human body, Cd accumulates in various organs with a long biological half-life (10-30 years) due in part to its low excretion rate (see for a comprehensive description the report of U.S. Department of Health and Human Services, 2012; Bocca et al., 2014; Choong et al., 2014; IARC, 2012). This metal has been classified as a human carcinogen by the International Agency for Research on Cancer (IARC), but the underlying mechanisms of action are complex and not completely known to date (IARC, 2012; Hartwig, 2013).

A powerful tool for mechanistic studies of carcinogenesis is represented by the Cell Transformation Assays (CTAs). The CTAs are the most advanced *in vitro* test for the prediction of human carcinogenicity induced by chemicals, in terms of standardization and validation (Vanparys et al., 2012), and are used since decades as *in vitro* methods for screening the potential carcinogenicity and for investigating the mechanisms of action of hazardous compounds (Combes et al., 1999; Corvi et al., 2012). In addition, these assays have been shown to closely model some key stages of the conversion of normal cells to malignant phenotypes, like the *in vivo* carcinogenic process (Landolph, 1985). In this regard, the CTA based on the use of C3H10T1/2Cl8 mouse embryo fibroblasts, which are among the suitable cells suggested by standard protocols (OECD, 2007), has been indicated as a useful model to elucidate the molecular mechanisms of cell transformation at the genomic and transcriptomic levels (Vasseur and Lasne, 2012). Upon chemical exposure, these cells undergo morphological transformation visualized by the formation of transformed cell

colonies (*foci*). The *foci* are recognised under a microscope and classified by standard features, such as deep basophilic staining, multilayered growth, random cell orientation at the edge of the *focus*, and invasiveness of the surrounding monolayer of normal cells (Landolph, 1985; OECD, 2007). These morphological features are related to molecular changes leading the cells to acquire fully malignant characteristics, which was demonstrated by their ability to yield tumours when injected into susceptible host animals (Reznikoff et al., 1973). The CTAs are a relatively simple technique, in comparison to the two-year bioassay with rodents (OECD, TG451), have the potential to analyse both genotoxic and some non-genotoxic chemicals, and support with the 3Rs principles of Replacement, Reduction and Refinement of experimental animals. Furthermore, they provide a tool for the comprehension of the mechanisms underlying the *in vitro* carcinogenic processes, which is still to be exploited. The latter represents a specific follow-up request of the European Union Reference Laboratory for Alternatives to Animal Testing, along with the automation of *foci* scoring, in order to increase throughput and reliability of CTAs, and to possibly include these assays in the regulatory carcinogenicity testing battery (EURL ECVAM, 2012; Creton et al., 2012).

The activation of the epidermal growth factor receptor (EGFR) pathway is one of the best characterized molecular mechanisms so far identified in the cell transformation process (Baselga, 2001; Venook, 2005; Immervoll et al., 2006), and has a central role in the pathogenesis and progression of different carcinoma types (Normanno et al., 2006). EGFR is a member of the tyrosine kinase ErbB receptor family, playing an important role in the regulation of cell growth, proliferation, and differentiation (Zhen, 2003; Liu, 2011). Upon binding of the epidermal growth factor (EGF) to its receptor (EGFR), two main downstream pathways can be activated: *1)* the Ras/Raf/mitogen-activated protein kinase (MAPK) signalling cascade (activated when the Erk protein is hyperphosphorylated), that drives pro-proliferative gene expression, cytoskeletal rearrangement, and increased cell proliferation, and *2)* the phosphoinositide-3-kinase (PI3K)/PTEN/AKT cascade (activated when Akt protein is hyperphosphorylated), which is

involved in cell survival and motility (Jorissen et al., 2003). The identification of possible EGFR pathways alterations may open the door to new therapies also in early phases of the development of several cancer types. Of high relevance, several drugs directly targeting either EGFR or a member of its downstream pathways have been developed or are under evaluation in clinical trials (www.clinicaltrials.gov).

The aim of the present study is the characterization of proliferative and survival behaviours in C3H10T1/2Cl8 cells transformed upon Cd exposure. Although it has been deeply studied in many cancer cell lines, EGFR activation has not been investigated in C3H10T1/2Cl8 mouse embryo fibroblasts so far, nor in other cell lines suitable for CTAs. Therefore, we focused on EGFR pathway as a starting point to identify the biochemical alterations underlying the morphological changes exploited in *foci* recognition and classification.

2. MATERIALS AND METHODS

2.1 Cells and culture conditions

The experiments were performed using contact-sensitive C3H10T1/2 clone 8 (C3H from here on) mouse embryonic fibroblasts (cell line ATCC, CCL 226 lot. n. 58078542). This cell line was chosen for its high sensitivity to carcinogenic compounds, its low spontaneous transformation rates, and because it represents one of the cell models suggested to be used in CTAs (OECD, 2007). The cells were stored in ampoules, frozen at –80°C with 10% sterile DMSO as a preservative. Cells at passages from 9 to 12 were used for cell transformation studies (OECD, 2007). Cells were cultured in Basal Medium Eagle (BME, Sigma Chemical Co., St. Louis, MO, USA) enriched with 10% heat-inactivated fetal bovine serum (FBS, Euroclone, Pero, Italy), 1% glutamine, 0.5% HEPES 2M and 25 μg/mL gentamicin (all purchased from Sigma) at 37°C in a humidified incubator supplied with a constant flow of 5% CO_2 in air throughout each experiment. Cells were routinely seeded in 100 mm Ø Petri dishes, the medium was changed every 3 days and cells were grown until 80% confluence

maximum was reached.

2.2. Chemicals

The stock solution (1 mM) of $CdCl_2$ (97% purity BDH Laboratory, Milan, Italy) was prepared in ultra-pure water (0.22 μm filtered Milli-Q water, Millipore, Vimodrone, Milan, Italy) and stored at 4°C. Stock solution of 12-O-tetradecanoylphorbol-13-acetate (TPA) (Sigma) was prepared in DMSO to a final concentration of 1 μg/μl. TPA was chosen as a well-known promoter agent (OECD, 2007**)**.

2.3 Cell transformation assay and isolation of the cells for biochemical characterization

C3H were seeded at a density of 800 cells/dish in 100 mm diameter Petri dishes, and exposed 24 h after seeding to 1 μM $CdCl_2$ for 24 hours. Previous Cell Transformation Assays performed by our group (Urani et al., 2009) on a wide range of $CdCl_2$ concentrations demonstrated that 1 μM $CdCl_2$, which is below the cytotoxicity threshold (IC_{50} of 2.4 μM), is able to induce the formation of transformed *foci*. Therefore, in the present work we have used a single concentration with the only aim to obtain transformed cells to be further isolated and characterized.

Samples treated with $CdCl_2$, were exposed 4 days after the treatment to 0.1 μg/ml TPA in DMSO. TPA addition was maintained throughout all the experiments. Cells exposed to 0.1 μg/ml TPA alone were used as controls. The negative controls consisted in the medium alone or the medium containing DMSO at the final concentration below the 0.1% (v/v) set by the OECD (OECD, 2007).

After 24 hours of treatment, the cells were rinsed twice with phosphate buffered saline (PBS) and fresh medium was added. The medium was changed weekly. Upon confluence (around the 3rd week), high serum (10% FBS) medium was substituted with low (5% FBS) serum medium. The samples were observed weekly under a light microscope throughout the duration of the assay (6 weeks) to check health cells status and *foci* formation. At the end of CTAs (6th week) Cd-

transformed *foci* and all needed controls were identified by microscopy examination, were scrape-harvested and re-seeded in 35 mm Ø Petri dishes for future biochemical characterization. All Petri dishes were then rinsed with PBS, fixed in absolute methanol for 10 min, and stained with 10% (v/v in distilled water) Giemsa solution, rinsed three times with distilled water and observed by light microscopy for *foci* scoring and classification, according to standard procedures.

All methodological details of CTAs with C3H cells are elsewhere described (Reznikoff et al., 1973; Landolph, 1985; OECD, 2007; Urani et al., 2009). In Figure 1, an outline of the experimental design is provided.

The following cell samples were collected at the end of CTAs and re-seeded (from here on cell clones) for a further characterization:

- CTR: cells from a normal monolayer of sample exposed to complete medium only
- TPA: cells from a monolayer exposed to TPA alone
- F1: cells from a fully transformed *focus* (Type III) after exposure to 1μM $CdCl_2$
- F2: cells from a *focus* classified as intermediate between Type II and III after exposure to 1μM $CdCl_2$
- F3: cells from a fully transformed *focus* (Type III) after exposure to 1μM $CdCl_2$
- MN3: cells from the contact-inhibited monolayer in the Petri dish where F3 was collected.

2.4 Morphological criteria for cell transformation

The CTAs rely on the evaluation of morphological changes in cell colonies (*foci*) through optical microscopy observation performed by a trained expert (Landolph, 1985, OECD 2007). In the C3H CTA, Type II and III *foci* are considered fully transformed and scored for the estimate of the transformation frequency (TF). When reinjected into syngenic animals, cells from Type II and Type III *foci* form tumours with a frequency of 50% and 80-90% respectively (Reznikoff, 1973; Male et

al., 1987). The scoring is based on standard morphological criteria (Reznikoff, 1973; Landolph, 1985): Type II are *foci* with extensive cellular piling into multilayers and mildly polar cells; Type III are *foci* with highly polar, fibroblastic and multilayered crisscrossed cells. Examples of a Type III *focus* obtained upon Cd exposure at the end of CTAs, and further morphological features are shown and described in Figure 2. Type I *foci*, although showing highly packed cells, are excluded from the estimate of the TF being characterized by a normal morphology.

2.5 Proliferation assays

Proliferation activity of each clone was assessed through two different assays, the first one aiming at the evaluation of the proliferation activity in term of cell count at consecutive time points, the second one focused on the morphological analysis of different clones at confluence.

In the first assay cell clones (CTR, TPA, MN3, F3, F1 and F2) were seeded (100.000 cell/35 mm Ø Petri dishes, 50.000 cells/ml) and harvested by trypsinization at 24, 48 and 72 hours after seeding. Aliquots (40 µl) of the cell suspension were diluted in isotonic solution and counted in a Coulter counter (Z1, Beckman Coulter Inc, CA, USA). All counts were expressed as number of cells/ml.

In the second assay, all cell clones were seeded at 100.000 cells/35 mm Ø Petri dishes (50.000 cells/ml) and left in culture until confluence was reached to test for their contact-inhibition properties. All dishes were then fixed in methanol for 10 min at room temperature, washed in distilled water, stained with 10% Giemsa for 10 min at room temperature and finally washed again in distilled water. All samples were viewed under a Zeiss Axioskop 40 microscope (5x objective magnification) and photographed with Axiovision 4.6 software (Zeiss, Oberkochen, Germany).

2.6 SDS-PAGE and Western blotting

All cell clones were harvested by trypsinization at 80% confluence, washed with ice-cold PBS and lysed in RIPA buffer (50 mM Tris-HCl pH 7.5, 150 mM NaCl, 1% NP-40, 0.5% sodium

deoxycholate, 0,1% SDS) containing proteases and phosphatases inhibitors and 1 mM PMSF (phenylmethylsulfonyl fluoride). After lysis on ice, homogenates were obtained by passing 5 times through a blunt 20-gauge needle fitted to a syringe and then centrifuged at 15,000 g for 30 min. Supernatants were analysed for protein content by the BCA protein assay (Smith et al., 1985).

SDS-PAGE and Western blotting were carried out by standard procedures (Laemmli, 1970). Sixty µg of proteins were separated on a 10% acrylamide/bis-acrylamide SDS-PAGE, transferred onto a nitrocellulose membrane (Millipore, Billerica, MA, USA), probed with the appropriated antibodies and visualized using ECL detection system (Millipore). Protein levels were quantified by densitometry of immunoblots using ScionImage software (Scion Corp., Frederick, MD, USA). The following primary antibodies were used (all purchased by Cell Signaling Technology, Danvers, MA, USA): anti EGFR (dilution 1:1000), phospho-EGFR (Tyr1068; dilution 1:1000), p44/42 MAPK (Erk1/2; dilution 1:1000), phospho-p44/42 MAPK (P-Erk1/2) (Thr202/Tyr204; dilution 1:1000), Akt (dilution 1:1000), phospho-Akt (Ser 473; dilution 1:1000), PTEN (dilution 1:1000), vinculin (dilution 1:1000). IgG HRP-conjugated secondary antibodies (purchased by Cell Signaling Technology, Danvers, MA, USA) were diluted 1:10000.

2.7 Statistical analysis

Data from proliferation assays were analysed as follows. The maximum value over 3-4 technical replicates was calculated for each block/time/clone tuple after recognizing that experimental errors in technical replicates may only be negative. The two blocks were both full factorial designs with 6 clones tested at 3 times, but they differed in the number of biological replicates, 3 in the first block and 2 in the second block. The final dataset comprises 83 observations because 6 x 3 = 18 clone-time treatments got 3 biological replicates in the first block (54 observations) and 2 biological replicates in the second block (36 observations), but 7 values were missing, thus 54 + 36 – 7 = 83 observations were available at the end of the experiment.

We decided to analyse count data fitting a general linear mixed-effects model (Pinheiro and Bates, 2000) to improve the estimate of variance and to better capture technical variability through a variance component. The sample size may be considered quite small for what regards the goal of estimating specific parameters for each time and each treatment. A joint model of all observations, by contrast, has the potential of reducing bias and of capturing further features of the data generating process, like technical variability, finally leading to more powerful tests.

Then, observed counts $Y_{e,c,t,j}$ are decomposed as follows:

$$Y_{e,c,t,j} = \mu + \alpha_e + \gamma_c + \beta_t + \theta_{c,t} + \varepsilon_{e,c,t,j} \quad \text{eq.1}$$

where *e* indicates a block, *c* refers to a clone, *t* to time and *j* to biological replicate within clone-time. Residuals are assumed to be independent normal variables $\varepsilon_{e,c,t,j} \sim N\left(0, \sigma^2_{e,c,t,j}\right)$ with the variance a power function of the expected value of the response Y, precisely:

$$\sigma^2_{e,c,t,j} = \sigma^2 \mu^{2\delta}_{e,c,t,j} \quad \text{eq.2}$$

where δ is a model parameter to be estimated. Right side of equation 1, mu is the mean value of the TPA clone (considered as the reference control), alpha is a random effect associated to blocks in the experiment, thus $\alpha_e \sim N\left(0, \sigma^2_\alpha\right)$ are normally distributed and independent; gammas are fixed effects representing departure of other clones from the mean value of TPA; betas are fixed effects due to time with respect to the 24hours; thetas are interactions between clone and time, therefore they capture specific behaviour of clones at different times (see supplementary material for details). Likelihood ratio test for the hypothesis of null interaction were also performed. Quantile-quantile plot of normalized residuals were checked out looking for evidences against the normality assumption of model residuals. Calculations were performed in R (R Core Team, 2015) using the nlme package (Pinheiro et al., 2015).

Densitometric data from Western blot analysis were analysed as follows. Each target (protein

analysed) for each cell clone was analysed in triplicates. Densitometric values for each clone and each target were normalized to the loading control (vinculin); in the case of phosphorylated targets, densitometric values were normalized to the value obtained for the total target protein.

Since values of Erk tot were missing in one replicate of Erk phosphorylation, model-based imputation was performed by regressing observed Erk tot on vinculin, then by estimating the expected value of Erk tot in the missing replicate given its observed values of vinculin. Robust estimates of model parameters were obtained under the assumption that residuals followed a Student-*t* distribution with small degree of freedom, that is a heavy-tailed distribution.

Values of fold change versus control, the TPA clone, were finally calculated after imputation of missing values TPA clone.

All clone-to-control contrasts were tested by Dunnet multiple comparison procedure applied to log-transformed fold-change data.

Calculations were performed in R (R Core Team, 2015) using the heavy package (Osorio, 2014) and multcomp package (Hothorn et al., 2008).

3. RESULTS

3.1 Cadmium exposure leads to cell transformation

In our experiments, dishes exposed to 1μM Cd (inducer)+TPA (promoter) showed a high number (20) of transformed *foci* leading to a high TF (TF=0.78). On the contrary, both negative control groups, CTR (samples with medium only) and TPA, never showed any Type II or Type III *focus*, thus resulting in a TF=0 the TF is expressed as a function of the average number of transformed *foci* per plate divided by the number of surviving cells, as suggested by standard protocols (OECD, 2007). Surviving cells are calculated in a preliminary cytotoxicity test (data not shown), according to standard protocols (OECD, 2007).

3.*2 Transformed foci have different proliferation rates*

Since changes in cell morphology and growth behaviour in culture represent typical features of transformed cells, morphological observation and cell proliferation rate estimates were carried out in all isolated clones (transformed and untransformed).

As expected, control samples (CTR) exhibited low cell density and the typical contact-inhibition of normal cells at confluence, when observed by optical microscopy (Figure 3, CTR). Normal cells from the contact-inhibited monolayer, harvested in Cd-treated plate (MN3), showed a morphology comparable to that of CTR with low density, and contact-inhibited cells (Figure 3, MN3). The TPA-treated samples (TPA) showed morphology comparable to CTR, although a slightly increased density could be observed (Figure 3, TPA). On the contrary, when cells from a fully transformed Type III *focus* (F3) were grown until confluence, they demonstrated a loss of contact-inhibition, and a dense growth, as shown by highly packed nuclei (Figure 3, F3). A dense growth was also observed in transformed cells of F1 and F2 clones, the latter also evidencing the formation of multilayered, piled-up areas typical of cells with loss of contact-inhibition (Figure 3, F1 and F2).

To quantify the proliferative behaviour, growth curves of all isolated clones were determined through cell counting, and subsequently analysed through a general linear mixed model specifically adapted.

Results of model fitting are summarized in Figure 4, left, where expected values for different clones at different times are plotted. Clones collected from transformed *foci*, like F1 and F2, deviate from the linear growth otherwise observed. 95% confidence intervals for the expected value of the response and original count values for 72 hours are shown (Figure 4, right) and they are all similar except for F1 clone showing a higher proliferation rate at 72 hours. While the likelihood ratio test for the hypothesis of null interactions between variables time and treatment was rejected ($p < 0.005$), the only significant interaction term in the final model (*t*-test) was clone F1 by time 72 hours ($p<0.05$). Quantile-quantile plot of normalized residuals did not show relevant evidences

against the assumption of normality for residuals.

3.3 Different transformed foci show activation of either proliferative or survival pathway

Since transformed cells are characterized by uncontrolled cell growth, we undertook the characterization of specific proliferative markers. The activation of EGFR pathways in different re-seeded cell clones was investigated. EGFR expression was found to be below the Western blot detection limit in all the cell clones (data not shown). However, intracellular mediators of proliferation (Erk, belonging to the MAPK pathway) and survival (Akt, belonging to the PI3K/PTEN/AKT pathway) were seen early deregulated in all the transformed clones. Protein activation was assessed through Western blotting of crude extracts, and immunodecoration was performed with antibodies recognizing either the phosphorylated or the total form of each protein.

As shown in Figure 5, F1 clone showed a significant ($p<0.001$) increase of Erk phosphorylation level compared to TPA clone, in agreement with its high proliferative activity. F2 clone showed a significant Erk phosphorylation level compared to TPA as well, although less marked than F1 ($p<0.05$). All other clones, including controls as well as F3 clone, did not show any significant and comparable phosphorylation levels. No significant differences in total Erk protein expression levels were found in all clones (Figure 5).

On the other hand, as reported in Figure 6, we observed an increase in Akt phosphorylation level (P-Akt) only in the F3 clone, compared to TPA. Although not statistically significant, this suggests a different activation trend in comparison with other transformed clones and controls.

No differences in total Akt protein expression levels were found in all clones (Figure 6).

To further investigate the deregulation of the PI3K/PTEN/AKT signalling cascade, we analysed its negative regulator, PTEN. Its protein levels (Figure 7) showed no alterations in all the cell clones.

4. **DISCUSSION**

With a long term aim of developing a quantitative and objective method of *foci* scoring and classification, our research group is working towards the automation of this step of the assay (Urani et al., 2009, 2013; Callegaro et al., 2015). Herewith we undertook a further step to meet EURL ECVAM recommendations, i.e. the molecular characterization of pathways involved in the complex process of cell transformation. Being the best characterized cancer activated pathway, EGFR and the activation of its downstream pathways were chosen as a starting point (Baselga, 2001; Venook, 2005; Immervoll et al., 2006). To the best of our knowledge, since the first pioneering study of Male and colleagues (1987), very few papers have addressed this issue; some authors have analysed the pathways involved in MCA+TPA-induced transformation in C3H10T1/2 cells (Priya et al., 2013), others have characterized gene expression profiles in BALB/c 3T3 transformed *foci* exposed to carcinogens or tumour promoting agents to identify a gene signature (Rohrbeck et al., 2010; Ao et al., 2010). Therefore, our work may significantly contribute to a knowledge advancement in this field.

It is noteworthy to remark that all fully transformed *foci* used herewith for the biochemical characterization (F1, F2 and F3) were formed at the end of the CTAs (6 weeks) upon the same chemical inducer ($CdCl_2$ 1µM, 24 hours), selected in previously performed experiments aimed at the identification of the carcinogenic dose-response (Urani et al., 2009). Cadmium-induced carcinogenesis is still a matter of study, although different mechanisms have been proposed or identified: e.g., the involvement of reactive oxygen species (ROS), the deregulation of cell growth and resistance to apoptosis (see Hartwig 2013, for a comprehensive review), and the interference with essential metals (Martelli et al., 2006; Urani et al., 2015). In the present study, the morphological analysis of *foci*-derived cell clones by optical microscopy showed in all instances a loss of contact-inhibition, as well as higher cell densities, compared to normal cells (Figure 3), all common features of transformed cells. However, proliferation rate analyses showed that only F1

clone displayed a significant increase, compared to control cells. The investigation of EGFR pathways, most commonly responsible for cell proliferation, confirmed these data. Our results indicate that EGFR itself does not seem to play any direct role in cadmium-induced *foci*: indeed, we were not able to detect EGFR protein expression levels neither in transformed nor in non-transformed clones, thus suggesting its marginal role in cadmium-induced transformation. This is in agreement with previously reported data in other cancer cells (Krasinskas, 2011). On the contrary, interesting considerations can be done on the analysis of EGFR downstream pathways, the MAPK axis (activated when Erk protein is hyperphosphorylated) and the PI3K/PTEN/AKT axis (activated when Akt is hyperphosphorylated). It is of high relevance that both these pathways have been found altered in cadmium-induced *foci*: either the ERK pathway, as in F1 cells and to a minor extent also in F2 cells, or the AKT pathway, as in F3 cell clone, were found to be activated. In particular, for F3 cell clone, we observed a trend in Akt phosphorylation levels, even though not statistically significant (sample size is equal to 3). In our samples, the alteration of Akt phosphorylation can be ascribed to Akt itself or to an upstream deregulation, but not to PTEN, a negative regulator of the PI3K/PTEN/AKT pathway, since we did not observe any significant change (decrease) in PTEN expression, when compared to TPA samples. F2 cells showed an increase in Erk phosphorylation despite its proliferation being comparable to controls. At the end of the CTA, F2 *focus* was classified by microscopy observation as intermediate (Type II/III) and morphological assessment of cell proliferation of its derived clone revealed spatial heterogeneity, i.e. the formation of multilayered, piled-up areas of cells. Thus we can consider F2 cell clone as having an intermediate phenotype reflecting the intermediate biochemical fingerprint observed for proliferation behaviour. Moreover, it is worth noticing that an increase in Akt phosphorylation was also detected in F3 clone, when compared to its own control (MN3 clone), representing untransformed cells growing as a monolayer in the same plate.

On the whole, our data suggest that F1 cell growth is supported by the activation of the ERK

pathway, leading to a high proliferation state. The same pathway is activated in F2 cell clone, although to a lower extent than in F1 cells. On the other hand, F3 cell clone shows a shift towards a survival mode, with the activation of the PI3K/PTEN/AKT pathway, paralleled by PTEN unaltered levels. The ability of cadmium to promote cell transformation through Erk and Akt signalling activation was recently reported in human lung epithelial cells, and was demonstrated to be mediated by ROS production (Jing et al., 2012). Further mechanisms of Erk and Akt signalling activation have been described and comprehensively reviewed (Choong et al., 2014). For instance, it is recognized that cadmium participates in many Ca^{2+}-dependent pathways in different cell types (e.g., skin fibroblasts, mesangial cells) due to its "ionic mimicry". The central role of cadmium in calcium mobilization and the changes in calmodulin and Ca^{2+}/calmodulin-dependent protein kinase II activation and their regulation of downstream signalling cascades, such as the Erk and Akt, have been described. Thus, the interplay of calcium and cadmium in mediating the transformation of C3H10T1/2 cells is a mechanism that deserves further studies.

It has to be highlighted that in our work, although both F3 and F1 clones were collected from fully transformed *foci*, as assessed by previously described morphological procedures of optical microscopy (Ao et al., 2010; Landolph, 1985), we have observed an activation of two different EGFR downstream pathways at a molecular level.

Our data clearly show that transformed *foci* classified on the basis of standard morphological features, may display different molecular profiles. The discovery of molecular alterations and/or markers of the *in vitro* cell transformation process will open the way to a deeper molecular characterization of *foci* and will lead to the identification of a number of quantitative parameters to be applied in CTAs. This characterization will be useful for the improvement of the assay, the comprehension of the *in vivo* carcinogenic process, and to fulfil with the specific requests of EURL ECVAM (2012).

A future expansion of the present study will be the molecular characterization of other receptor

tyrosine kinase pathways: in fact, our data, showing a deregulation of the MAPK and of the PI3K/PTEN/AKT pathways (which are shared by a number of receptor tyrosine kinases) and the absence of EGFR deregulation, clearly indicate that other receptor tyrosine kinases (such as HER2, HER3, HER4), which are expressed at different levels in various cell lines (Normanno et. al, 2006) may be involved in cadmium-induced *foci*.

Conclusions

In conclusion, we have demonstrated that cell clones derived from transformed *foci* obtained after the same treatment and classified by trained experts on the basis of standard morphological features (Ao et al., 2010), are characterized by different molecular pathways, survival or proliferation, both leading to uncontrolled cell growth (see Figure 8 for a sum up of the results). As known, typical hallmarks of cancer include, among others, a sustained signalling for proliferation, immortalization, resistance to cell death, and evasion of growth suppression. Accumulated evidence suggests that the cellular and molecular processes of the *in vivo* multistage carcinogenesis and the *in vitro* cell transformation are similar, and that the CTAs closely mimic the *in vivo* conversion of normal cells into the transformed phenotype (Combes et al., 1999; Sakai, 2007). Thus, the molecular characterization of cells from *foci* carrying a transformed phenotype is a key tool for CTAs improvement as well as crucial for the comprehension of the *in vivo* process, to investigate possible therapies and chemo-preventive properties of compounds. Our data along with those from the literature (Corvi et al., 2012; Urani et al., 2013; Annys et al., 2014) suggest that the CTAs should be further improved for their implementation in a regulatory context within a wider approach as the Integrated Testing Strategy (ITS) for the prediction of carcinogenic potential in agreement with the 3Rs principles.

Conflict of interest statement

None of the authors have any conflicts of interest.

Acknowledgments

CU acknowledges the partial support by Fondo di Ateneo (University of Milano Bicocca), and the European Commission. The Authors acknowledge Dr Claudio Procaccianti for the contribution in the CTAs assessment and isolation of cell clones.

References

Annys, E., Billington, R., Clayton, R., Bremm, K.D., Graziano, M., McKelvie, J., Ragan, I., Schwarz, M., van der Laan, JW., Wood, C1., Öberg, M., Wester, P., Woodward, KN., 2014. Advancing the 3Rs in regulatory toxicology – Carcinogenicity testing: Scope for harmonisation and advancing the 3Rs in regulated sectors of the European Union. Reg. Toxicol. Pharmacol. 69, 234-242.

Ao, L., Liu, J.Y., Liu, W.B., Gao, L.H., Hu, R., Fang, Z.J., Zhen, Z.X., Huang, M.H., Yang, M.S., Cao, J., 2010. Comparison of gene expression profiles in BALB/c 3T3 transformed *foci* exposed to tumor promoting agents. Toxicol. In Vitro 24, 430-438.

Baselga, J., 2001. The EGFR as a target for anticancer therapy-focus on cetuximab. Eur. J. Cancer 37, S16-22.

Bocca, B., Pino, A., Alimonti, A., Forte, G., 2014. Toxic metals contained in cosmetics: A status report. Reg. Toxicol. Pharmacol. 68, 447-457.

Callegaro, G., Stefanini, F.M., Colacci, A., Vaccari, M., Urani, C., 2015. An improved classification of foci for carcinogenicity testing by statistical descriptors. Toxicol. In Vitro, 29, 1839-1850.

Combes, R., Balls, M., Curren, R., Fischbach, M., Fusenig, N., Kirkland, D., Lasne, C., Landolph, J., LeBoeuf, R., Marquardt, H., McCormick, J., Müller, L., Rivedal, E., Sabbioni, E., Tanaka, N., Vasseur, P., Yamasaki, H., 1999. Cell transformation assays as predictors of human carcinogenicity. ATLA 27, 745–767.

Corvi, R., Aardema, M.J., Gribaldo, L., Hayashi, M., Hoffmann, S., Schechtman, L., Vanparys, P., 2012. ECVAM prevalidation study on *in vitro* cell transformation assays: General outline and conclusion of the study. Mutat. Res. 744, 12-19.

Creton, S., Aardema, M.J., Carmichael, P.L., Harvey, J.S., Martin, F.L., Newbold, R.F., O'Donovan, M.R., Pant, K., Poth, A., Sakai, A., Sasaki, K., Scott, A.D., Schechtman, L.M., Shen, R.R., Tanaka, N., Yasaei, H., 2012. Cell transformation assays for prediction of carcinogenic potential: state of the science and future research needs. Mutagenesis 27, 93-101.

EURL ECVAM, 2012. Recommendation on three Cell Transformation Assays using Syrian Hamster Embryo Cells (SHE) and the BALB/c 3T3 Mouse Fibroblast Cell Line for In Vitro Carcinogenicity Testing. Available at https://eurl-ecvam.jrc.ec.europa.eu/eurl-ecvam-recommendations/EURL-ECVAM%20-Recommendation.pdf

Hartwig, A., 2013. Metal interaction with redox regulation: an integrating concept in metal carcinogenesis? Free Rad. Biol. Med. 55, 63-72.

Hothorn, T., Bretx, F., Westfall, P., 2008. Simultaneous Inference in General Parametric Models. Biom. J. 50, 346-363.

IARC, 2012. International Agency for Research on Cancer. A review on human carcinogens: arsenic, metals, fibers and dusts. In IARC Monographs on the evaluation of carcinogenic risks to humans. (121-141) 100C Lyon, France.

Immervoll, H., Hoem, D., Kugarajh, K., Steine S.J., Molven A., 2006. Molecular analysis of the EGFR-RAS-RAF pathway in pancreatic ductal adenocarcinomas: lack of mutations in the BRAF and EGFR genes. Virchows Arch. 448, 788-796.

Jing, Y., Liu, L-Z., Jiang, Y., Zhu, Y., Lan Guo, N., Barnett, J., Rojanasakul, R., Agani, F., Jiang, B-H., 2012. Cadmium increases HIF-1and VEGF expression through ROS, ERK, and AKT signalling pathways and induces malignant transformation of human bronchial epithelial cells. Toxicol. Sci. 125, 10-19.

Jorissen, R.N., Walker, F., Pouliot, N., Garrett T.P., Ward C.W., Burgess A.W., 2003. Epidermal growth factor receptor: mechanisms of activation and signalling. Exp. Cell Res. 284, 31-53.

Krasinskas, A.M., 2011. EGFR signaling in colorectal carcinoma. Patholog. Res. Int. 2011, 932932.

Landolph, J.R., 1985. Chemical transformation of C3H10T1/2Cl8 mouse embryo cells: historical background, assessment of the transformation assay, and evolution, and optimization of the transformation assay protocol. In T. Kakunaga, H. Yamasaki (Eds.), IARC, Scientific Publication n. 67 (185-198). IARC, Lyon, France.

Leammli, U.K., 1970. Cleavage of structural proteins during the assembly of the head of bacteriophage T4. Nature 227, 680-685.

Liu, Y.C., Yen, H.Y., Chen, C.Y. Chen C.H., Cheng P.F., Juan Y.H., Chen C.H., Khoo K.H., Yu C.J., Yang P.C., Hsu T.L., Wong C.H., 2011. Sialylation and fucosylation of epidermal growth factor receptor suppress its dimerization and activation in lung cancer cells. Proc. Natl. Acad. Sci. U S A 108, 11332-11337.

Male, R., Bjerkvig, R., Lillehaug, J.R., 1987. Biological and biochemical characterization of cell lines derived from initiation-promotion transformed C3H10T1/2 cells. Carcinogenesis 8, 1375-1383.

Martelli, A., Rousselet, E., Dycke, C., Bouron A., Moulis J.M., 2006. Cadmium toxicity in animal cells by interference with essential metals. Biochimie 88, 1807–1814.

Normanno, N., De Luca, A., Bianco, C., Strizzi, L., Mancino, M., Maiello, M. R., Carotenuto, A., De Feo, G., Caponigro, F., Salomon, D.S., 2009. Epidermal growth factor receptor (EGFR) signaling in cancer. Gene 366, 2-16.

OECD, 2007. Detailed review paper on cell transformation assays for detection of chemical carcinogens. Series on testing and assessment, n. 31. ENV/JM/MONO(2007)18.

OECD. 2009. Test Guideline 451 – Carcinogenicity studies. OECD Guidelines for the Testing of Chemicals, OECD, Paris. Available athttp://www.oecd-ilibrary.org/environment/test-no-451-

carcinogenicity-studies_9789264071186-en.

Osorio, F., 2014. Heavy: Package for robust estimation using heavy-tailed distributions. R package version 0.2-35. http://cran.r-project.org/package=heavy.

Pinheiro, J.C., Bates, D.M., 2000. Mixed-Effects Models in S and S-PLUS, Springer.

Pinheiro, J., Bates, D., DebRoy, S., Sarkar, D. and R Core Team, 2015. nlme: Linear and Nonlinear Mixed Effects Models. R package version 3.1-120, http://CRAN.R-project.org/package=nlme.

Priya, S., Nigam, A., Bajpai, P., Kumar, S., 2013. Dysregulation of pathways involved in the processing of cancer and microenvironment information in MCA+TPA transformed C3H/10T1/2 cells. In Vitro Cell. Dev. Biol. Anim. 49, 295-305.

R Core Team, 2015. R: A language and environment for statistical computing. R Foundation for Statistical Computing, Vienna, Austria. http://www.R-project.org/.

Reznikoff, C.A., Bertram, J.S., Brankow, D.W., Heidelberger, C., 1973. Quantitative and qualitative studies of chemical transformation of cloned C3H Mouse Embryo Cells sensitive to postconfluence inhibition of cell division. Cancer Res. 33, 3239-3249.

Rohrbeck, A., Salinas, G., Maaser, K., Linge, J., Salovaara S., Corvi, R., Borlak, J., 2010. Toxicogenomics applied to *in vitro* carcinogenicity testing with Balb/c 3T3 cells revealed a gene signature predictive of chemical carcinogens. Toxicol. Sci. 118, 31-41.

Sakai, A., 2007. BALB/c 3T3 cell transformation assays for the assessment of chemical carcinogenicity. AATEX 14, 367-373.

Scion Image for Windows, Scion Corporation. Available at http://scion-image.software.informer.com/

Smith, P.K., Krohn, R.I., Hermanson, G.T., Mallia, A.K., Gartner F.H., Provenzano, M.D., Fujimoto, E.K., Goeke, N.M., Olson, B.J., Klenk, D.C., 1985. Measurement of protein using bicinchoninic acid. Anal. Biochem.150, 76-85.

Urani, C., Stefanini, F.M., Bussinelli, L., Melchioretto, P., Crosta, G.F., 2009. Image analysis and

automatic classification of transformed *foci*. J. Microsc. 234, 269-279.

Urani, C., Corvi, R., Callegaro, G., Stefanini, F.M., 2013. Objective scoring of transformed foci of BALB/c 3T3 cell transformation assay by statistical image descriptors. Toxicol. In Vitro 27, 1905–1912.

Urani, C., Melchioretto, P., Bruschi, M., Fabbri, M., Sacco, M.G., Gribaldo, L., 2015. Impact of cadmium on intracellular zinc levels in HepG2 cells: quantitative evaluations and molecular effects. BioMed Res. Int. 2015, 949514.

U.S. DEPARTMENT OF HEALTH AND HUMAN SERVICES, Public Health Service Agency for Toxic Substances and Disease Registry, 2012. Toxicological profile for cadmium.

Vanparays, P., Corvi, R., Aardema, M.J., Gribaldo, L., Hayashi, M., Hoffmann, S., Schechtman, L., 2012. Application of *in vitro* cell transformation assays in regulatory toxicology for pharmaceuticals, chemicals, food products and cosmetics. Mut. Res. 744, 111-116.

Vasseur, P., Lasne, C., 2012. OECD Detailed Review Paper (DRP) number 31 on Cell Transformation Assays for detection of chemical carcinogens: main results and conclusions. Mut. Res. 744, 8-11.

Venook, AP., 2005. Epidermal growth factor receptor-targeted treatment for advanced colorectal carcinoma. Cancer 10, 2435-2446.

Zhen, Y., Caprioli, R.M., Staros, J.V., 2003. Characterization of glycosylation sites of the epidermal growth factor receptor. Biochemistry 42, 5478-5492.

554 **Figure captions**

555

556 **Figure 1. Outline of the experimental design**.

557 A C3H10T1/2 CTA was performed and clones of transformed and untransformed cells were
558 isolated and characterized. Briefly, C3H cells were seeded at a density of 800 cells/dish in Petri
559 dishes, and exposed, 24 hours after seeding to 1 μM $CdCl_2$ for 24 hours. After 4 days cells were
560 exposed to 0.1 μg/ml 12-O-tetradecanoylphorbol-13-acetate (TPA), a known tumour promoter.
561 Controls were the cells exposed to DMSO, or to TPA alone. At the end of CTA (6^{th} week) some
562 Cd-transformed *foci* and all needed controls were observed under microscope, scrape-harvested and
563 re-seeded in 35 mm Ø Petri dishes for future biochemical characterization. Then, all Petri dishes
564 were methanol-fixed and Giemsa-stained for the assessment of the transformation frequency.

565 **Figure 2. Type III *focus.***

566 Example of different areas of a Type III *focus* formed at the end of a CTA (6^{th} weeks) induced by 1
567 μM $CdCl_2$ exposure, followed by TPA addition. The *focus* shows the typical morphological features
568 of transformation: deep basophilic staining and multilayering of transformed cells, the invasiveness
569 into the surrounding monolayer of normal contact-inhibited cells (upper right part of A, star) and
570 vortexes formation (B) with polarized and spindle shaped cells with flattened nuclei (C, D).
571 Magnification: A, B 32x; C, D 100x.

572 **Figure 3. Cell morphology evaluation.**

573 Clones from normal cells (CTR, TPA, MN3) and transformed *foci* (F1, F2, F3) were observed by
574 optical microscopy after fixing and Giemsa staining. The typical contact-inhibition at confluence is
575 displayed by normal cells, although TPA shows a slighter increase of cell density.
576 On the contrary, clones from transformed *foci* show a loss of contact-inhibition with tightly packed
577 nuclei and the formation of highly dense and piled-up regions. Magnification 50X.

578

Figure 4. Cell proliferation evaluation.

CTR, TPA, MN3, F3, F1 and F2 cell clones were seeded at 50.000 cells/ml and harvested by trypsinization at 24, 48 and 72 h after seeding. On the left, the expected values (empty circles) of clones at each time are estimated by a linear mixed-effects model. On the right, bars represent 95% confidence intervals of expected values for clones at time 72h (***p-value <0.05), while small dots represent original counts at time 72h .

Figure 5. Western blotting analysis of Erk activation.

A) Representative Western blotting performed on crude extracts, using anti-P-Erk and anti-Erk antibodies. Vinculin was used as a loading control. The experiments were performed in triplicate. B) Determination of phosphorylation rate by densitometric analysis was performed with Scion Image Software. Values are calculated as the P-Erk/total Erk ratio; each ratio is normalized on P-Erk/total Erk ratio of TPA treated control cells. Points and whiskers in (a), (c), (e), (g) and (i) represent respectively the means and confidence intervals for each fold ratio of each clone. In addition, bars and whisker in (b), (d), (f), (h) and (j) represent respectively means and standard errors for each fold ratio of each clone (** p-value <0.005, *** p-value <0.001).

Figure 6. Western blotting analysis of Akt activation.

A) Representative Western blotting performed on crude extracts, using anti-P-Akt and anti-Akt antibodies. Vinculin was used as loading control. The experiments were performed in triplicate.

B) Determination of phosphorylation rate by densitometric analysis was performed with Scion Image Software. Values are calculated as the P-Akt/total Akt ratio; each ratio is normalized on P-Akt/total Akt ratio of TPA treated control cells. Points and whiskers in (a), (c), (e), (g) and (i) represent respectively the means and confidence intervals for each fold ratio of each clone. In addition, bars and whisker in (b), (d), (f), (h) and (j) represent respectively means and standard errors for each fold ratio of each clone.

Figure 7. Western blotting analysis of PTEN protein level.

A) Representative Western blotting performed on crude extracts, using anti-PTEN antibody. Vinculin was used as loading control. The experiments were performed in triplicate.

B) Densitometric analysis of total protein content was performed with Scion Image Software. Data are expressed as fold changes compared to TPA treated control cells. Points and whiskers in (a), (c), (e), (g) and (i) represent respectively the means and confidence intervals for each fold ratio of each clone. In addition, bars and whisker in (b), (d), (f), (h) and (j) represent respectively means and standard errors for each fold ratio of each clone.

Figure 8. **Graphical representation of the results**. In two different clones of cadmium-induced transformed cells, two different pathways were found to be activated. Cells belonging to the clone called F3 showed an activation of the PI3K/Akt/mTOR pathway, known to be related to cell survival, while cells belonging to clone called F1 are supported by proliferative signals, due to the activation of MEK/ERK1,2 axis.

Figure(s)

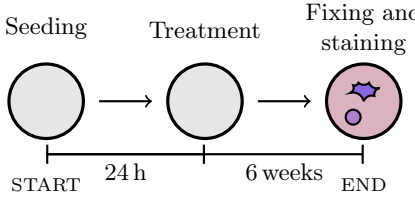
Seeding
Treatment
Fixing and staining
START
24 h
6 weeks
END

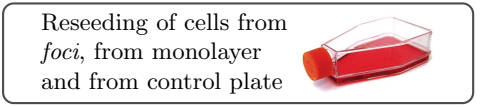
Reseeding of cells from *foci*, from monolayer and from control plate

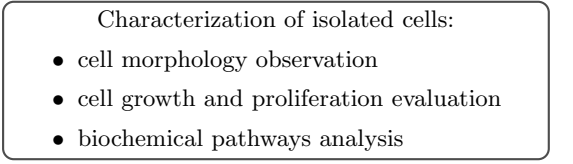
Characterization of isolated cells:
• cell morphology observation
• cell growth and proliferation evaluation
• biochemical pathways analysis

Figure 2

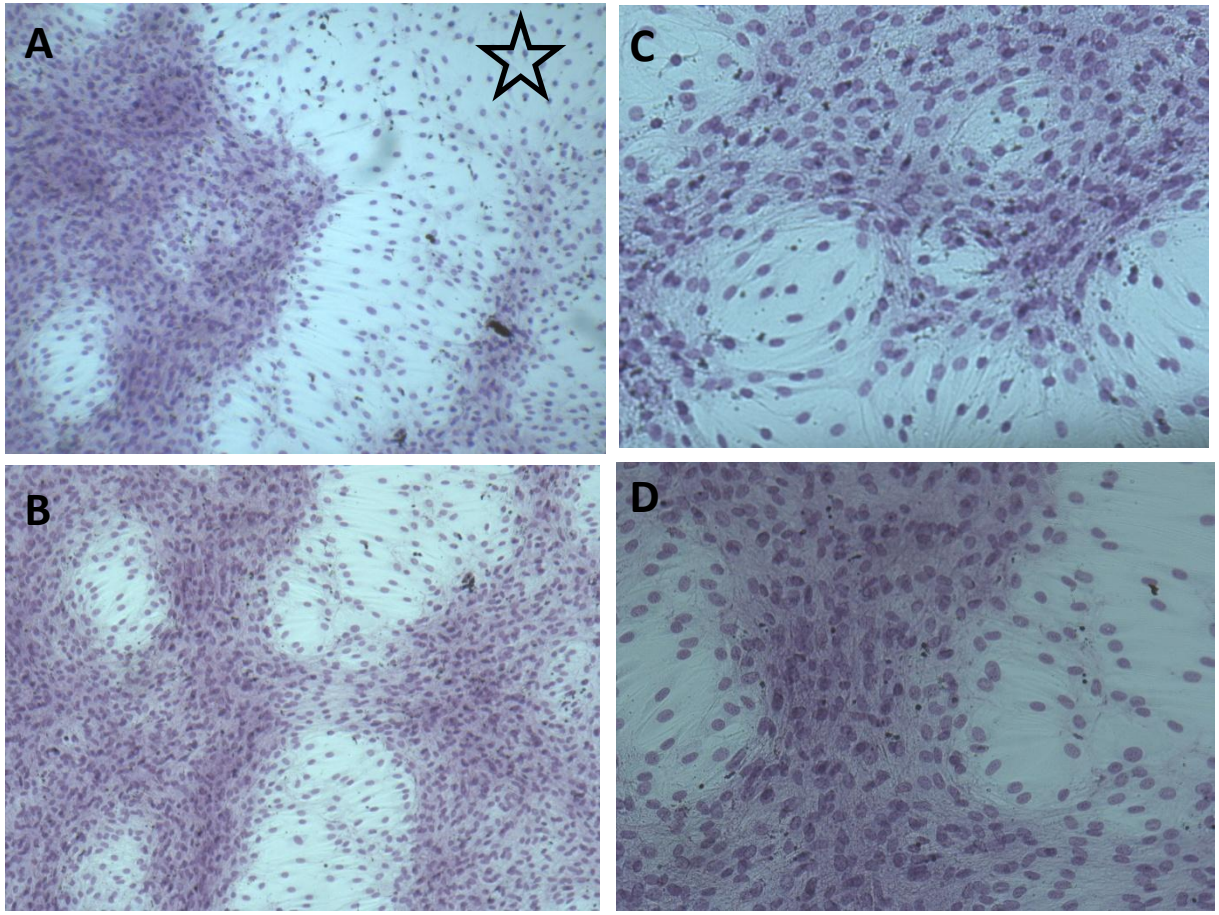

Figure(s)

Figure 3

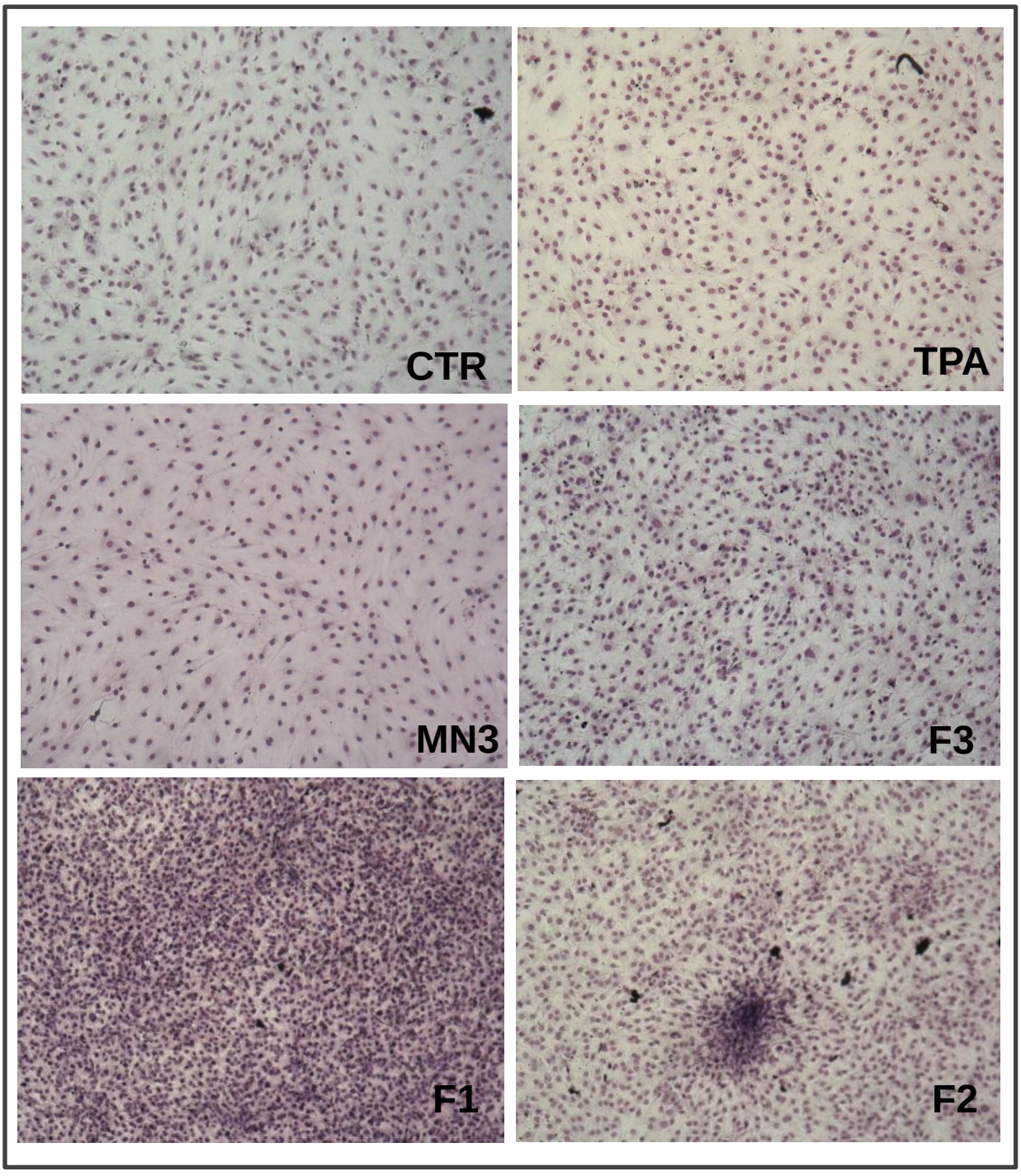

Figure(s)

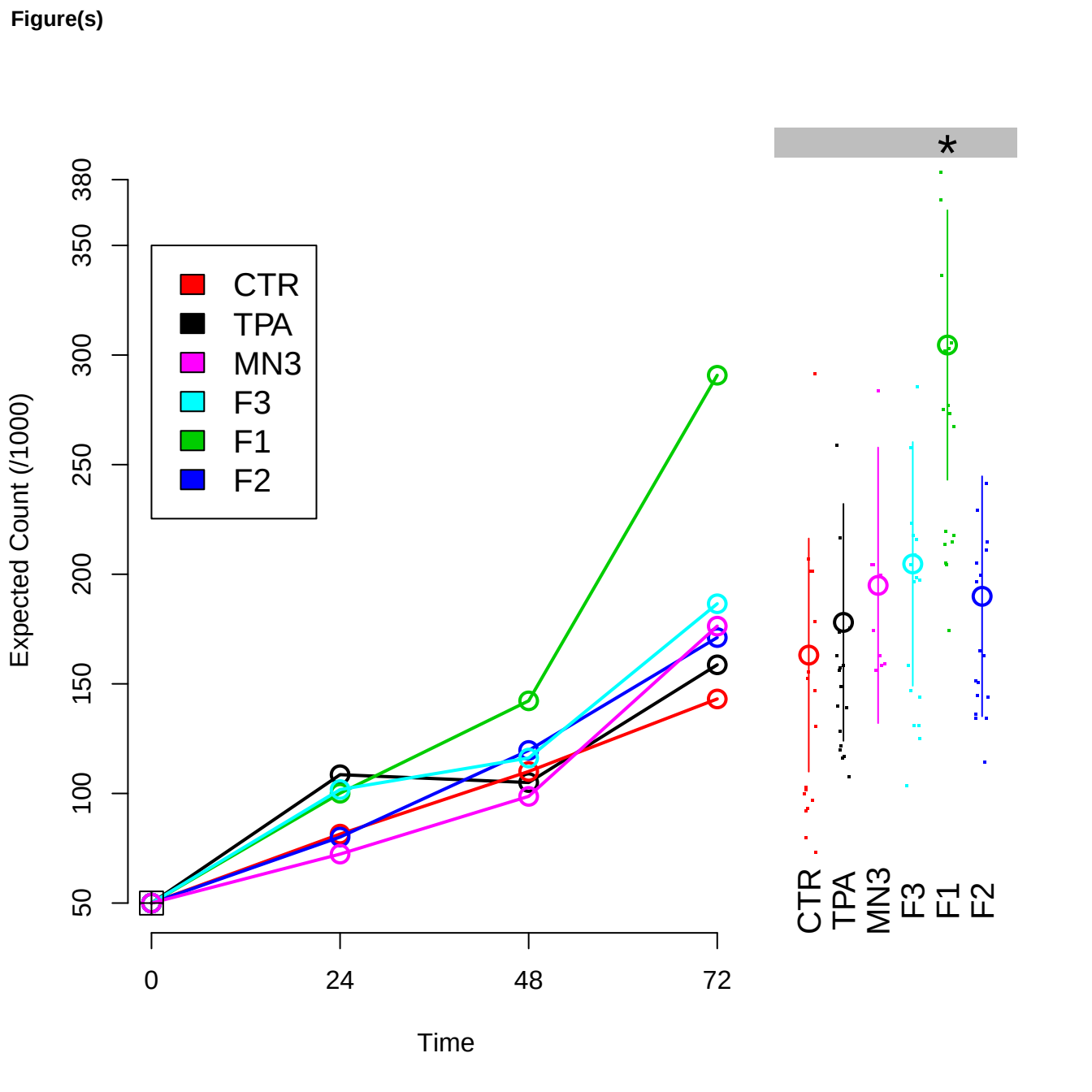
Expected Count (/1000)
50
100
150
200
250
300
350
380
0
24
48
72
Time
CTR
TPA
MN3
F3
F1
F2
*
CTR
TPA
MN3
F3
F1
F2

Figure(s)
Click here to download high resolution image

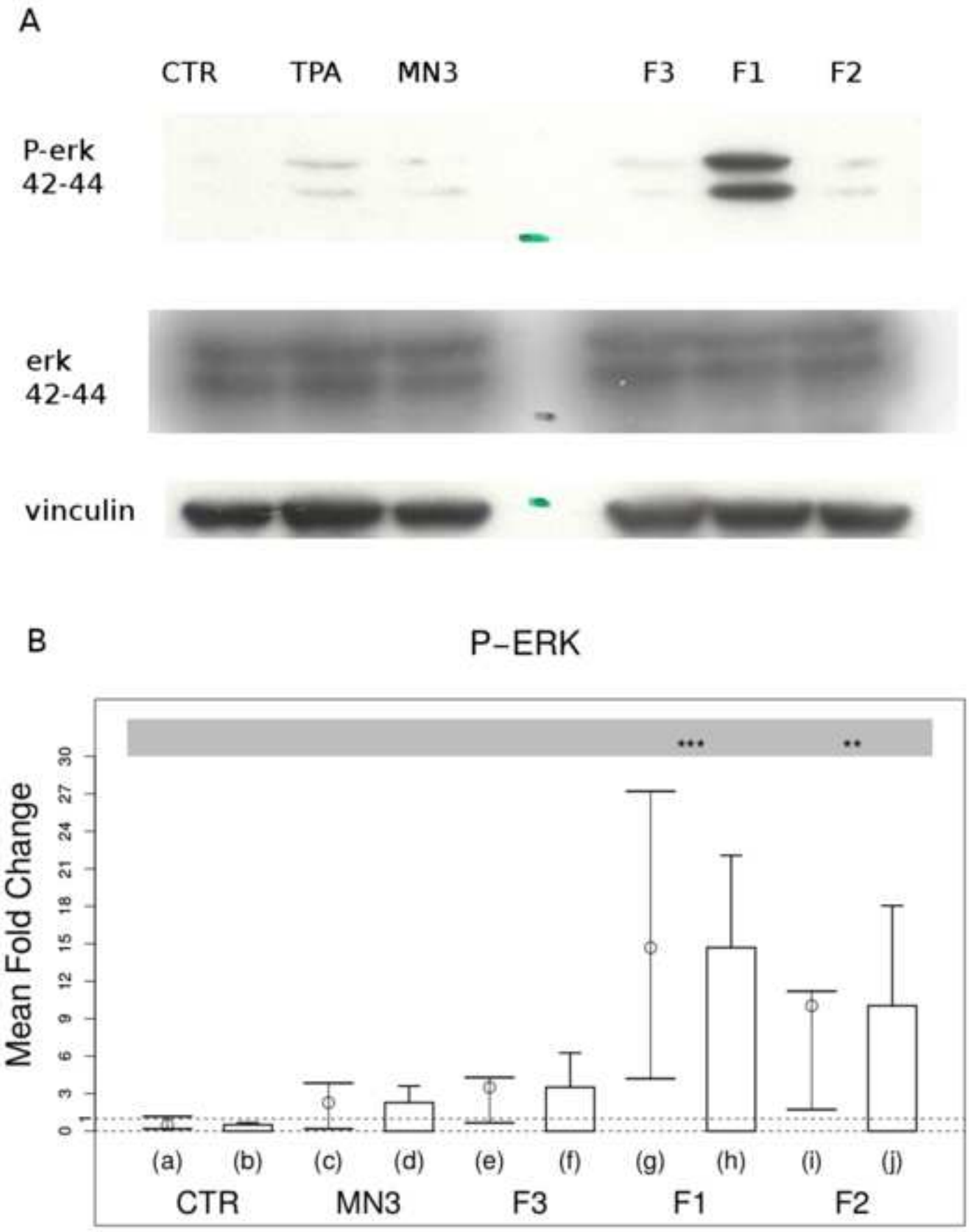

Figure(s)
Click here to download high resolution image

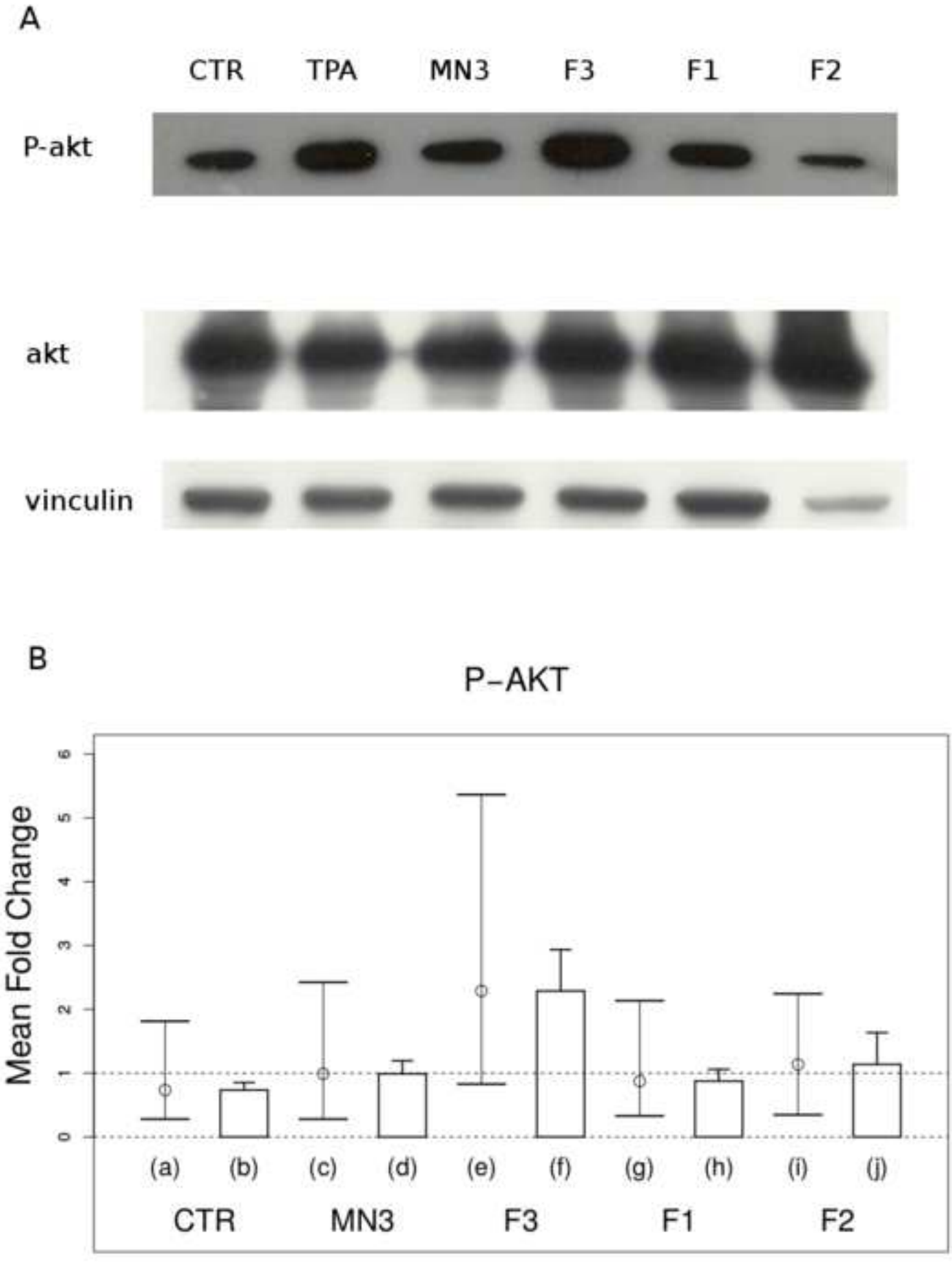

Figure(s)
Click here to download high resolution image

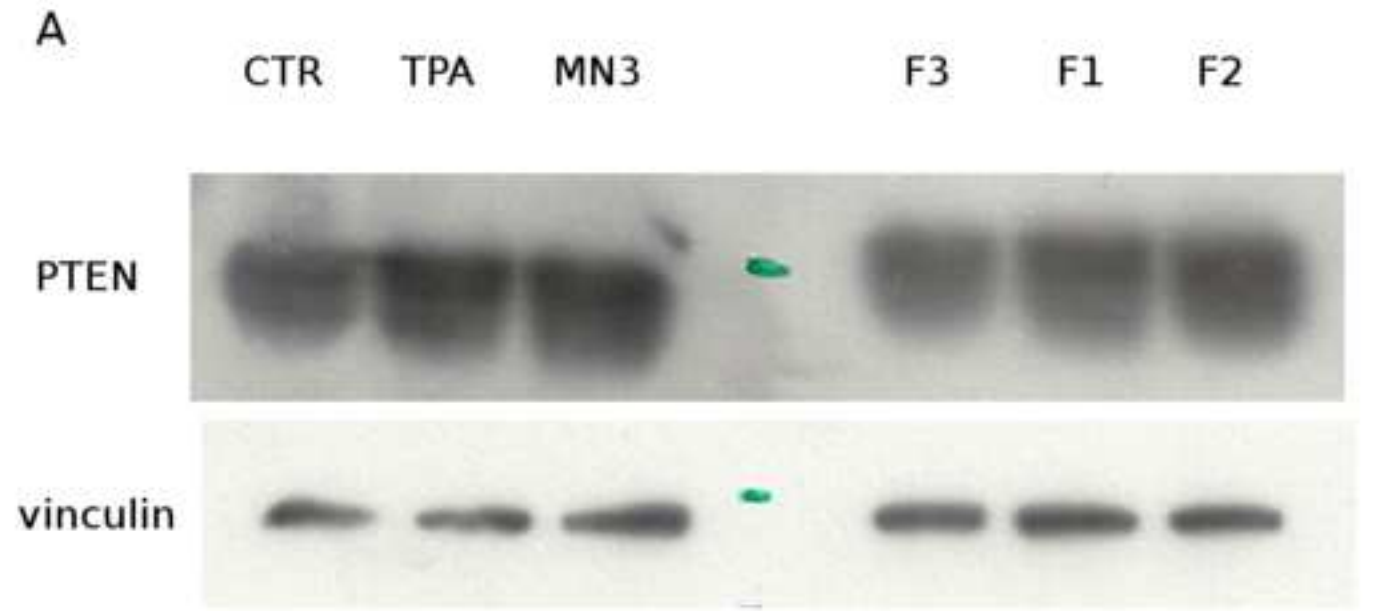

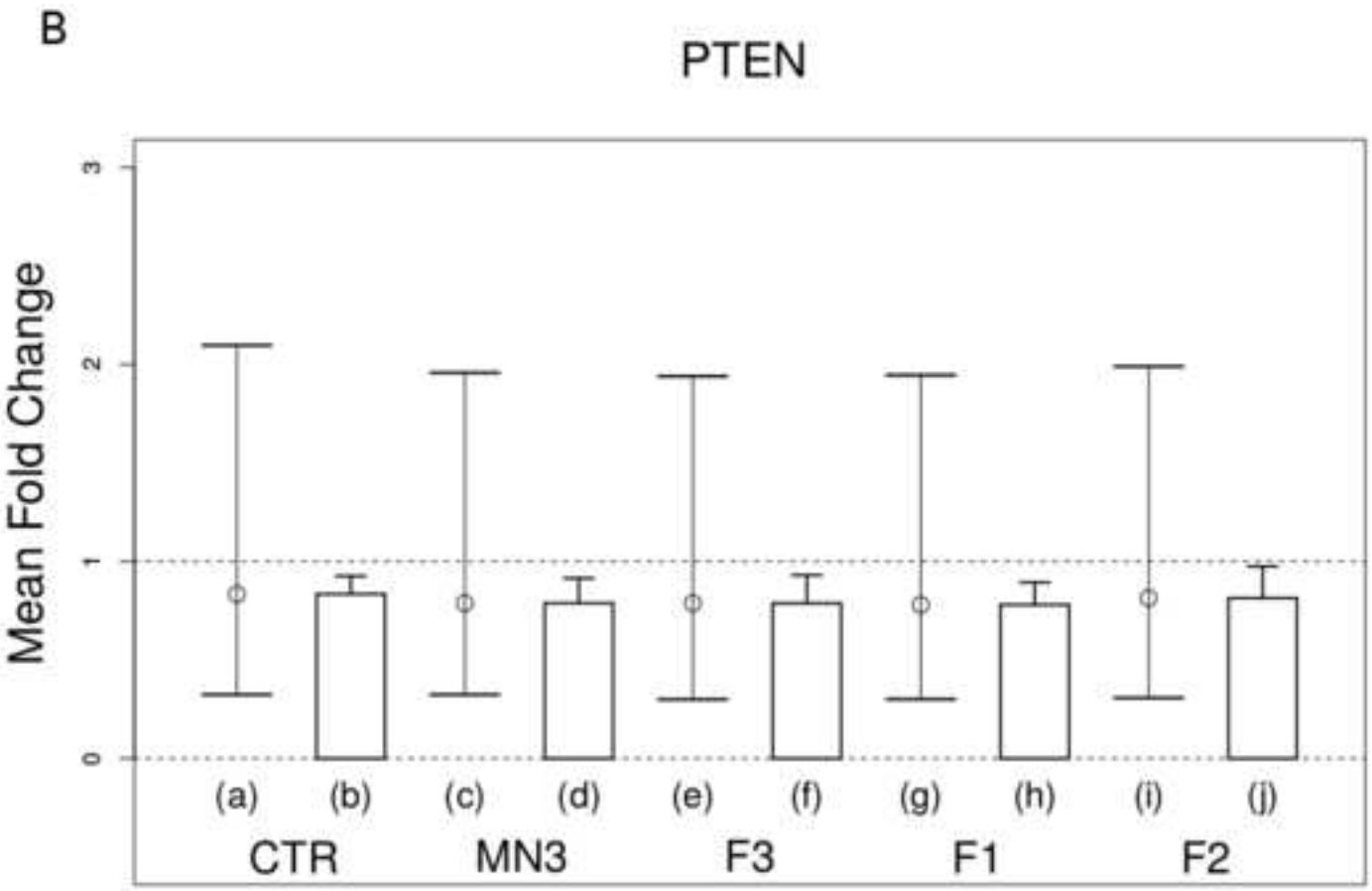

Figure(s)

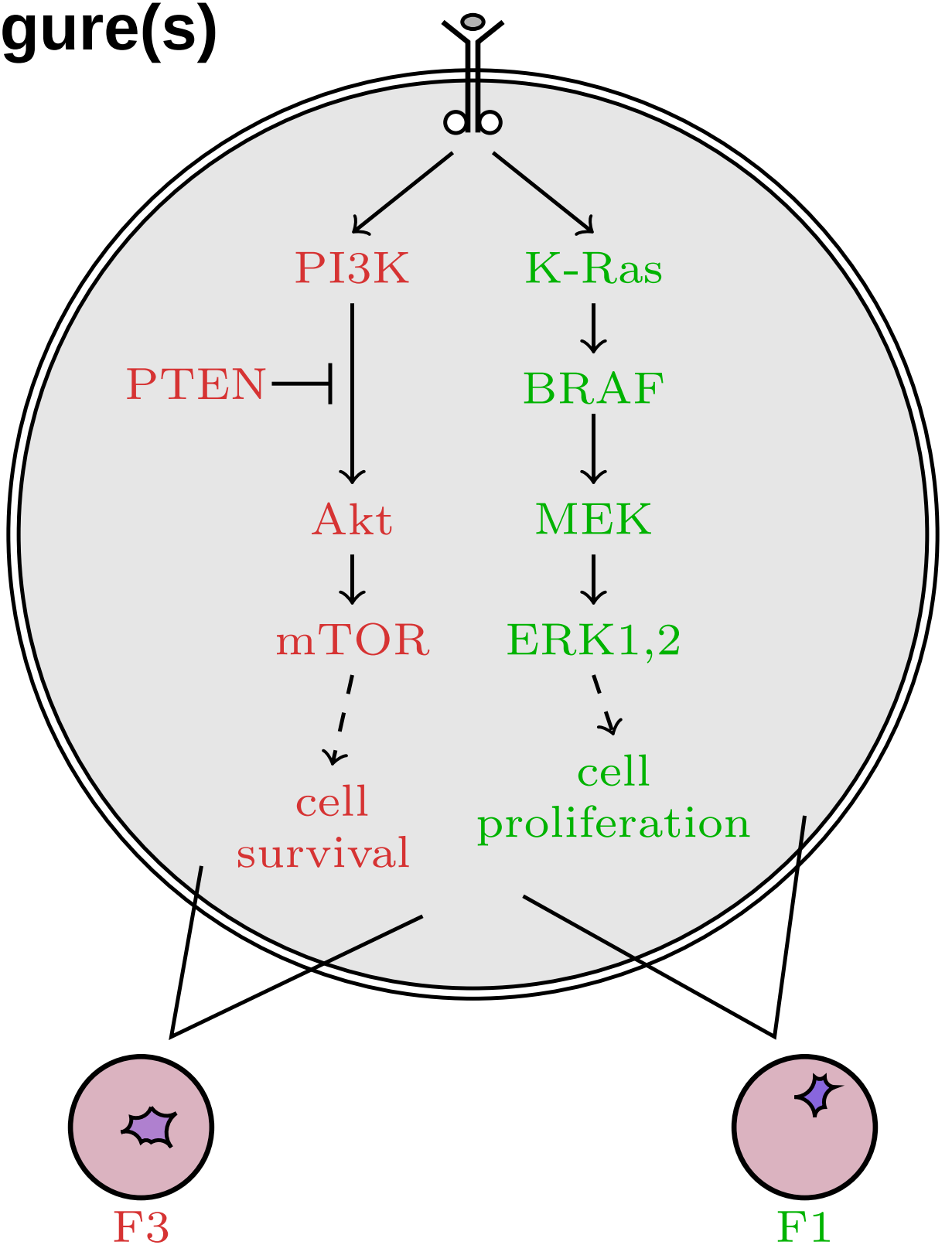
PI3K
K-Ras
PTEN
BRAF
Akt
MEK
mTOR
ERK1,2
cell
survival
cell
proliferation
F3
F1